PERGAMON

International Journal of Multiphase Flow 27 (2001) 1199–1226

International Journal of Multiphase Flow

www.elsevier.com/locate/ijmulflow

A fast Eulerian method for disperse two-phase flow

Jim Ferry [a,*], S. Balachandar [b]

[a] *Center for Simulation of Advanced Rockets, University of Illinois at Urbana-Champaign, Urbana, IL 61801, USA*
[b] *Department of Theoretical and Applied Mechanics, University of Illinois at Urbana-Champaign, Urbana, IL 61801, USA*

Received 26 March 2000; received in revised form 14 November 2000

Abstract

We propose a variant of the Eulerian method for two-phase flow that is valid for small particle response time τ. For small τ, the particle velocity field $\mathbf{v}(\mathbf{x},t)$ approaches a unique, equilibrium field, independent of initial conditions. A precise inequality is derived specifying how small τ must be for this to occur. When it does, $\mathbf{v}(\mathbf{x},t)$ depends only on local fluid quantities (velocity and its spatial and temporal derivatives), and may be expressed as an expansion in τ. We derive an expansion which generalizes those of previous researchers. The first-order truncation of this expansion may be computed efficiently, so by using it to approximate $\mathbf{v}$, the method avoids the need to solve additional partial differential equations, and therefore is much faster than the standard Eulerian method. Results from a direct numerical simulation of turbulent channel flow indicate that this first-order approximation of $\mathbf{v}$ is sufficiently accurate. Static tests performed at one time-instance show the actual velocities of particles evolved in a Lagrangian fashion are estimated well by evaluating the first-order approximation of $\mathbf{v}$ at the particles' positions. In particular, turbophoresis is represented accurately. Dynamic tests examine the effect of using the first-order approximation of $\mathbf{v}$ to evolve particles. The distribution of particles evolved in this way differs little from that of particles evolved using the standard Lagrangian method, indicating that static errors do not accumulate over time. In particular, the approximate method accurately captures preferential concentration in regions of high strain and low vorticity. Analogous results hold for bubbles. Therefore, for sufficiently small particles of any density, the first-order approximation to $\mathbf{v}$ is accurate, so the proposed variant of the Eulerian method is both accurate and fast.

Keywords: Two-phase flow; Eulerian; Fast Eulerian; Channel flow; Turbulent channel flow; Direct numerical simulation

* Corresponding author.

0301-9322/01/$ - see front matter
PII: S0301-9322(00)00069-0

1. Introduction

There are a variety of techniques for the numerical simulation of two-phase flows. To highlight the need for different techniques, let us imagine a monodisperse, particle-laden flow with density ratio (of the dispersed to the continuous phase) of $\rho = 10^3$ and a volume fraction (of the dispersed phase) of $c = 10^{-4}$. What simulation technique should we use in this situation? The answer depends critically on the size (or, equivalently, response time τ) of the particles compared to the characteristic time-scale of the surrounding flow. A range of techniques are shown in Fig. 1. If particles are very small, they can be considered to move with the fluid and be spatially well mixed. We may then treat the flow as single phase, with a modified density of $1 + (\rho - 1)c$. For instance, in the above example effective density will be approximately 1.1 times the fluid density. For a larger particle diameter, the particle velocity can no longer be considered to be equal to the fluid velocity, and c begins to exhibit spatial variations. Nevertheless, the particles are still well represented by a continuum model, so one may treat the particles in an Eulerian fashion. This entails the evolution of particle concentration field $c(\mathbf{x}, t)$ and a particle velocity field $\mathbf{v}(\mathbf{x}, t)$ along with the fluid velocity field $\mathbf{u}(\mathbf{x}, t)$. The derivation of the evolution for $c(\mathbf{x}, t)$ and $\mathbf{v}(\mathbf{x}, t)$ is complicated by the fact that they represent an average over all possible particle velocities at $(\mathbf{x}, t)$. Eight partial differential equations (PDEs) now need to be evolved in time instead of just four for fluid velocity and pressure. In a polydisperse system, the concentration and particle velocity fields must be defined separately for each particle size to be considered, in which case the Eulerian approach for particles can become quite expensive.

For particles larger still, the Eulerian method ceases to be appropriate; either because the number density of particles is so low that the continuum model ceases to apply; or because the inertia of the particles is too large for the particle velocity to be well represented by a unique field $\mathbf{v}(\mathbf{x}, t)$. Fortunately, if the particles are large, then there are fewer of them for a given loading. In this case, we may use a Lagrangian approach for the particles, in which the particles are tracked individually. This method is typically costlier than the Eulerian method; although the actual cost depends on the number of particles to be tracked. However, it has an advantage over the Eulerian method in that it allows two particles with different velocities to be in the same fluid volume (and to collide, if this is implemented). There is no averaging over all possible velocities at a point $(\mathbf{x}, t)$. It has the disadvantage that the back-effect of the particle on the fluid is somewhat difficult to account for. Finally, as the particle size increases further, the flow around the particle becomes complicated, and the back-effect of the particle on the fluid becomes so important that the simple parameterization implicit in the Lagrangian method fails. In this case, one needs to resort to a single-phase simulation of the carrier fluid, but with the exclusion of immersed particles. The cost of simulating the flow details around each sphere typically makes this method far more expensive than the Lagrangian method.

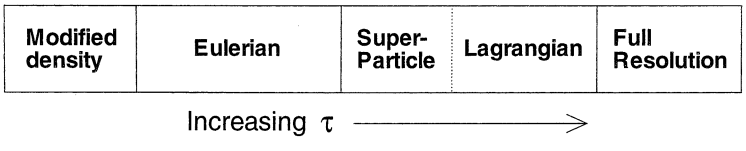

Fig. 1. Particle evolution methodologies.

Although we observe a general trend of increased expense as particle size increases (for fixed ρ and c), there are regimes where the trend is the reverse. The expense of the Lagrangian method increases as the particle size decreases (since the number of particles to track increase). Thus, there is a problem at the boundary between of Eulerian and Lagrangian methods. Here, particles are too big to be treated in Eulerian fashion, but too numerous for Lagrangian techniques. Necessity has produced so-called *super-particle* methods in which each computational particle represents many real particles. But there is concern about the accuracy of these methods. There is also a problem at the boundary between the Eulerian and "modified density" methods. The cost of the Eulerian method is largely independent of particle size, but when the particles get too small, the evolution equation for $\mathbf{v}(\mathbf{x}, t)$ becomes stiff, necessitating a smaller time-step than the fluid phase requires.

This paper examines a method for stimulating two-phase flows in the small-τ portion of the regime in which the Eulerian method applies. We pursue a suggestion originally (to our knowledge) exploited by Maxey (1987): that the particle velocity field can be expressed in terms of the fluid velocity as an expansion in particle time-scale. Such an expansion was recently considered by Druzhinin (1995) and Druzhinin and Elghobashi (1998, 1999). The important feature of the expansion is that the particle velocity field $\mathbf{v}(\mathbf{x}, t)$ can be explicitly evaluated in terms of $\mathbf{u}(\mathbf{x}, t)$ and its spatial and temporal derivatives, without solving additional PDEs. Thus only one additional PDE for the concentration field, $c(\mathbf{x}, t)$, need be solved for particles of certain size range. Bypassing the need to solve an equation for $\mathbf{v}(\mathbf{x}, t)$ (an equation which becomes stiff for small τ), this approach eliminates a small time-scale from the problem. Otherwise, there is a time-step constraint of the form $\Delta t < k\tau$ for some constant k. The method is much faster than the traditional Eulerian method and for further reference we term it the *fast Eulerian* method (see Fig. 2). It forms a natural bridge between the modified density method and the traditional Eulerian method as will be seen later in Section 4.2.

Here we extend the formal expansion (Maxey, 1987; Druzhinin, 1995) to include the effects to added mass, Basset history, and Saffman lift forces on the particle. More importantly, we evaluate the accuracy of the fast Eulerian approach in a turbulent channel flow by comparing the statistics the approach yields with "exact" Lagrangian statistics. Since the Eulerian approximation is expressed as an expansion in particle time-scale, this comparison will also allow us to judge the rate of convergence and, from a practical point of view, determine how much imporvement in prediction can be achieved with the first few terms of the expansion.

The Eulerian approach certainly has limitations. For example, the motion of a baseball through air cannot be described in terms of an expansion in the velocity of the surrounding air. The Eulerian approximation to particle velocity is an expansion in particle time-scale. Convergence can be expected only for small particles and bubbles with small time-scale compared to that of the surrounding flow. The expansion is likely to diverge for particles, such as the baseball, with a

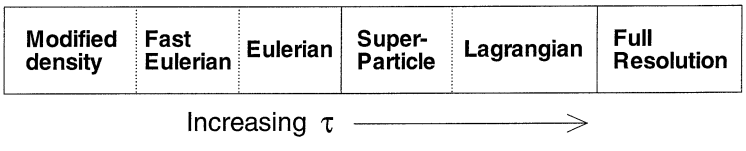

Fig. 2. The fast Eulerian method's niche.

larger time-scale. Furthermore, a Eulerian velocity field for the particle assumes a unique velocity for the particle a given $\mathbf{x}$ and t. However, the inherent Lagrangian nature of particle motion can result in different velocities for different particles at the same $\mathbf{x}$ and t, depending on the history of their motion. Truly, one requires a particle distribution function, $f(\mathbf{x}, \mathbf{v}, t)$, in phase space to account for the multi-valuedness of the particle velocity. In the limit of particle time constant, $\tau \to 0$ a unique particle velocity field is appropriate. On the other hand, the initial conditions of very large particles persist for such a long time that it is inappropriate to speak of a unique field description for particle velocity. It is then natural to ask if there is a particle time-scale (non-dimensionalized with respect to the surrounding flow) below which an Eulerian description with unique particle velocity field is appropriate. Here we provide such a criterion, which is similar to one recently obtained by Meiburg et al. (1999) for the existence of unique velocity for particles settling in a unidirectional flow. These theoretical issues are addressed in Section 2. In Section 3 we present numerical comparison of the Lagrangian and fast Eulerian (Eulerian expansion) approaches for the case of turbulent channel flow. Finally in Section 4 we consider implications of such an Eulerian expansion for particle distribution and for two-way coupling.

2. Theory

2.1. The particle velocity field for small τ

Maxey (1987) and later Druzhinin (1995) considered the following equation of motion:

$$\frac{\mathrm{d}\mathbf{v}}{\mathrm{d}t} = \frac{1}{\tau}(\mathbf{u} - \mathbf{v}) + \mathbf{g} \tag{1}$$

for particles subjected to only viscous drag and gravity forces. In the above equation the particle time-scale, τ, is given by $\tau = a^2/(3\beta\nu)$, where β is the density ratio parameter to be defined below, and $\mathbf{g}$ is acceleration due to gravity. Now if an Eulerian particle velocity field $\mathbf{v}(\mathbf{x}, t)$ is assumed, then from the above Lagrangian equation of motion the following expansion for particle velocity field is obtained:

$$\mathbf{v} = \mathbf{u} - \mathbf{a}\tau + \left(\frac{\mathrm{D}\mathbf{a}}{\mathrm{D}t} + \mathbf{a}\cdot\nabla\mathbf{u}\right)\tau^2 + \mathrm{O}(\tau^3), \tag{2}$$

where $\mathrm{D}/\mathrm{D}t$ is the total derivative following the fluid element, $\mathrm{d}/\mathrm{d}t$ is the total derivative following the particle, and $\mathbf{a}$ is the modified acceleration, $\mathbf{a} = \mathrm{D}\mathbf{u}/\mathrm{D}t - \mathbf{g}$. Maxey (1987) used the first-order version of this equation to explain the preferential accumulation of dense particles in regions of low vorticity and high strain. The expansion was extended later to second-order in the analytical work of Druzhinin (1995). Here we want to first extend this formal expansion to include other effects, such as added-mass, Basset history and Saffman lift forces.

The Maxey–Riley equation without the Faxén correction (Maxey and Riley, 1983), using Auton's form for the added mass (Auton et al., 1988), plus the Saffman lift term (Saffman, 1965) takes the following form:

$$m_p \frac{d\mathbf{v}}{dt} = 6\pi a\mu(\mathbf{u}-\mathbf{v}) + m_f \frac{D\mathbf{u}}{Dt} + \frac{1}{2}m_f\left(\frac{D\mathbf{u}}{Dt} - \frac{d\mathbf{v}}{dt}\right) + (m_p - m_f)\mathbf{g} + \frac{6\pi a^2\mu}{\sqrt{\nu}}\frac{d^{1/2}}{dt^{1/2}}(\mathbf{u}-\mathbf{v}) + \frac{9J_\infty}{\pi}a^2\sqrt{\frac{\mu\rho_f}{|\boldsymbol{\omega}|}}(\mathbf{u}-\mathbf{v})\times\boldsymbol{\omega}. \tag{3}$$

The first term on the right is Stokes drag, which can be modified to include higher Reynolds number correction if needed. The second term on the right is the fluid acceleration force, which will be felt even in the absence of the particle. The third term is the added-mass force, the fourth is gravity, and the fifth is the Basset history term. (Appendix A contains details on the usage of $d^{1/2}/dt^{1/2}$ in the Basset history term.) The last term on the right is the Saffman lift term; here it is written in terms of $J_\infty \approx 2.255$ so that one may substitute some version of the function $J(\varepsilon)$ if a more accurate expression for lift is desired (for details see McLaughlin, 1991; Wang et al., 1997). Here $\boldsymbol{\omega}$ is the vorticity of the external flow surrounding the particle.

The above general equation of particle motion can be written in a compact form by introducing the density ratio parameter, $\beta = 3/(2\rho+1)$, where $\rho = \rho_p/\rho_f$. Then

$$\frac{d\mathbf{v}}{dt} = \frac{1}{\tau}(\mathbf{u}-\mathbf{v}) + \beta\frac{D\mathbf{u}}{Dt} + (1-\beta)\mathbf{g} + \sqrt{\frac{\beta}{\tau}}\mathscr{L}[\mathbf{u}-\mathbf{v}], \tag{4}$$

where $\mathscr{L}$ is a linear operator defined as

$$\mathscr{L}[\mathbf{f}] = \sqrt{3}\frac{d^{1/2}\mathbf{f}}{dt^{1/2}} + \frac{3\sqrt{3}J_\infty}{2\pi^2\sqrt{|\boldsymbol{\omega}|}}\mathbf{f}\times\boldsymbol{\omega}. \tag{5}$$

We solve for $\mathbf{v}$ in terms of $\mathbf{u}$ when the particle time-scale τ is small. Since we expect $\mathbf{v}$ to be equal to $\mathbf{u}$ for $\beta = 1$, and to differ by $O(\tau)$ otherwise, we write

$$\mathbf{v} = \mathbf{u} - (1-\beta)\tau\mathbf{q}. \tag{6}$$

We may now express the time derivative following the particle in terms of the derivative following the fluid:

$$\frac{d}{dt} = \frac{D}{Dt} - (1-\beta)\tau\mathbf{q}\cdot\nabla. \tag{7}$$

Thus,

$$\left(1 + \sqrt{\beta\tau}\mathscr{L} + \tau\frac{d}{dt}\right)(\mathbf{u}-\mathbf{v}) = (1-\beta)\tau\left(\frac{D\mathbf{u}}{Dt} - \mathbf{g} - \tau\mathbf{q}\cdot\nabla\mathbf{u}\right), \tag{8}$$

and so,

$$\mathbf{q} = \left(1 + \sqrt{\beta}\tau\mathscr{L} + \tau\frac{d}{dt}\right)^{-1}(\mathbf{a} - \tau\mathbf{q}\cdot\nabla\mathbf{u}), \tag{9}$$

where, as above, $\mathbf{a} = D\mathbf{u}/Dt - \mathbf{g}$. We now invert the operator

$$\left(1 + \sqrt{\beta\tau}\mathscr{L} + \tau\frac{d}{dt}\right)^{-1} = 1 - \sqrt{\beta\tau}\mathscr{L} - \tau\left(\frac{D}{Dt} - \beta\mathscr{L}^2\right) + O(\tau^{3/2}), \tag{10}$$

so

$$\mathbf{q} = \mathbf{a} - \sqrt{\beta\tau}\mathscr{L}\mathbf{a} - \tau\left(\frac{\mathrm{D}\mathbf{a}}{\mathrm{D}t} + \mathbf{a}\cdot\nabla\mathbf{u} - \beta\mathscr{L}^2\mathbf{a}\right) + \mathrm{O}(\tau^{3/2}) \tag{11}$$

and finally,

$$\mathbf{v} = \mathbf{u} + (1-\beta)\left(-\mathbf{a}\tau + \sqrt{\beta}\mathscr{L}\mathbf{a}\tau^{3/2} + \left(\frac{\mathrm{D}\mathbf{a}}{\mathrm{D}t} + \mathbf{a}\cdot\nabla\mathbf{u} - \beta\mathscr{L}^2\mathbf{a}\right)\tau^2 + \mathrm{O}(\tau^{5/2})\right). \tag{12}$$

The definition of $\mathscr{L}$ involves $\mathrm{d}^{1/2}/\mathrm{d}t^{1/2}$, which is a derivative following the particle. One may replace this with $\mathrm{D}^{1/2}/\mathrm{D}t^{1/2}$ in the above, absorbing the difference into the $\mathrm{O}(\tau^{5/2})$ term. The above is a formal expansion for the particle velocity in terms of the fluid velocity field and is valid even with the inclusion of added-mass, Basset history and lift forces.

With the above general formalism several appropriate limits can be taken to obtain the corresponding simplified form of the particle velocity field. In the limit when the external gravitational force represented by $\mathbf{g}$ is dominant (i.e., $\mathbf{g} \approx \mathrm{O}(\mathbf{u}/\tau)$, Eq. (12) can be rewritten in terms of the terminal velocity, $\mathbf{w} = (1-\beta)\mathbf{g}\tau$, as

$$\mathbf{v} = \mathbf{u} + \mathbf{w} - \sqrt{\beta}\mathscr{L}\mathbf{w}\tau^{1/2} - \left((1-\beta)\frac{\mathrm{D}\mathbf{u}}{\mathrm{D}t} + \frac{\mathrm{D}\mathbf{w}}{\mathrm{D}t} + \mathbf{w}\cdot\nabla(\mathbf{u}+\mathbf{w}) - \beta\mathscr{L}^2\mathbf{w}\right)\tau + \mathrm{O}(\tau^{3/2}). \tag{13}$$

Since $\mathbf{g}$, and hence $\mathbf{w}$, is generally constant over space and time, the Basset component of $\mathscr{L}\mathbf{w}$ is 0, so the Saffman lift force is the dominant source of the relative velocity's deviation from the terminal velocity, and it occurs at order $\tau^{1/2}$ as follows:

$$\mathbf{v} = \mathbf{u} + \mathbf{w} + \frac{3J_\infty}{2\pi^2}\sqrt{\frac{3\beta\tau}{|\boldsymbol{\omega}|}}\boldsymbol{\omega}\times\mathbf{w} + \mathrm{O}(\tau). \tag{14}$$

In the dense-particle limit ($\beta \to 0$), the Saffman lift terms become unimportant and to $\mathrm{O}(\tau)$ one can recover the expansion in Maxey (1987):

$$\mathbf{v} = \mathbf{u} + \mathbf{w} - \left(\frac{\mathrm{D}\mathbf{u}}{\mathrm{D}t} + \mathbf{w}\cdot\nabla\mathbf{u}\right)\tau + \mathrm{O}(\tau^2). \tag{15}$$

Further discussion in the paper will pertain to small particles, for which the fast Eulerian approach is applicable. Also, we shall restrict our attention to the case $\mathbf{g} \approx \mathrm{O}(\mathrm{D}\mathbf{u}/\mathrm{D}t)$. For further discussion we shall also ignore $\mathscr{L}$, which means our results will hold up to $\mathrm{O}(\tau^{3/2})$ when $\beta = \mathrm{O}(1)$ – this step is mainly to avoid complications arising from the evaluation of Basset history term. Hence, the equation of interest reduces to

$$\mathbf{v} = \mathbf{u} + (1-\beta)\left(-\mathbf{a}\tau + \left(\frac{\mathrm{D}\mathbf{a}}{\mathrm{D}t} + \mathbf{a}\cdot\nabla\mathbf{u}\right)\tau^2 + \mathrm{O}(\tau^3)\right). \tag{16}$$

With $\beta = 0$ the above is essentially the same as the equation considered by Druzhinin (1995). A significant feature of all the above forms of the expansion is that particle velocity is simply related to the local fluid velocity and its local spatial and temporal derivatives. Thus in any computational procedure, once $\mathbf{u}(\mathbf{x},t)$ is evaluated, the corresponding particle velocity field can be obtained relatively easily without solving additional PDEs. Furthermore, it is easy to obtain different

particle velocity fields for particles of different sizes (or, in other words, for different time constants τ). Of course, there are questions regarding convergence and the asymptotic nature of the above expansion, especially as a function of increasing τ. Also the uniqueness of the above expansion can be questioned. These issues will now be addressed.

2.2. Uniqueness of the particle velocity field

The formal manipulations of the previous section are based on the assumption that there is a unique Eulerian field representation for the particle velocity $\mathbf{v}(\mathbf{x},t)$, given a fluid velocity field, $\mathbf{u}(\mathbf{x},t)$. However, for any given fluid velocity $\mathbf{u}$, the corresponding particle velocity is clearly dependent on its initial condition. Two different particle velocity fields, $\mathbf{v}_1$ and $\mathbf{v}_2$, can evolve differently in the same fluid field $\mathbf{u}(\mathbf{x},t)$ provided they started with different initial conditions. This dependence on initial conditions is likely to persist for at least some finite period of time. Therefore the question of whether a unique particle velocity field can be defined needs to be addressed only beyond an initial transient period. We can anticipate a unique particle velocity field for sufficiently small particles, where how small the particles need to be is likely to depend on the flow field. It can be expected that for particles whose characteristic time-scale τ is smaller than a certain characteristic time scale of the fluid, any two initially different particle velocity fields $\mathbf{v}_1$ and $\mathbf{v}_2$ converge exponentially fast. For such particles we may speak of a single field $\mathbf{v}$ once the transients arising from the initial conditions decay.

We have derived a rigorous condition for particle velocity fields to converge. Let $R_1(t)$ be a material volume for the velocity field $\mathbf{v}_1(\mathbf{x},t)$. We define

$$E(t) = \sup_{\mathbf{x}\in R_1(t)} |\mathbf{v}_1(\mathbf{x},t) - \mathbf{v}_2(\mathbf{x},t)|^2. \tag{17}$$

Then $E(t) \leqslant E(0)e^{-kt}$ for some $k > 0$ provided all eigenvalues of $1/2(\nabla\mathbf{v}_2 + (\nabla\mathbf{v}_2)^{\mathrm{T}})$ over the region swept out by $R_1(t)$ are greater than $-1/\tau$. Provided this condition is satisfied a unique equilibrium particle velocity field can be assumed to exist. Any initial deviation from equilibrium will decay exponentially, and the particle velocity will entrain to a unique velocity field. Appendix B contains the details and proof of this convergence theorem.

The convergence of particle velocity fields should not be confused with the convergence of individual particle paths. Suppose $\mathbf{v}_1(\mathbf{x},t_0)$ and $\mathbf{v}_2(\mathbf{x},t_0)$ differ slightly, and $-1 \ll \sigma_2\tau$ (σ_2 is the maximal compressional strain of the flow: maximal over the entire flow domain and time – see Appendix B for details), guaranteeing that $\mathbf{v}_1$ and $\mathbf{v}_2$ are converging quite quickly. Place two tracer particles at $\mathbf{x}_0$, one with initial velocity $\mathbf{v}_1(\mathbf{x}_0,t_0)$, the other with velocity $\mathbf{v}_2(\mathbf{x}_0,t_0)$. The velocity fields will quickly entrain to the same field, however, at all later time the particles will be at different positions. It is well established that even simple flows can produce chaotic particle paths. In a turbulent flow it is virtually certain that the two particles paths will diverge exponentially. The result in this section is about the convergence of particle velocity fields, not of individual particles.

2.2.1. A related result

The above convergence theorem is similar to that of a special case considered by Meiburg et al. (1999) for the existence of unique settling velocity for particles falling in a two-way coupled,

unidirectional flow. Their example, somewhat restated for the present discussion, is as follows: Consider the case of particles falling in still air under the action of gravity. For simplicity let particle inertia, Stokes drag, and gravity be the only forces on the particle. The equation of motion for the vertical velocity, v, of the particle can then be written as

$$\frac{\mathrm{d}v}{\mathrm{d}t} = \frac{1}{\tau}(w - v), \tag{18}$$

where w is the terminal velocity of the particle. Integrating the above equation twice we get the following solution for the velocity $v(t)$ and the position $y(t)$ of the particle:

$$v(t) = v_0 e^{-t/\tau} + w(1 - e^{-t/\tau}), \tag{19}$$

$$y(t) = y_0 + wt + \tau(v_0 - w)(1 - e^{-t/\tau}), \tag{20}$$

where y_0 is the initial position of the particle and $v_0(y_0)$ is the initial velocity of the particle, which is here considered to be a function of the initial particle position. If we consider the particle velocity to be a function of both y and t, the condition of uniqueness can be stated thus: $v(y,t)$ must be a single-valued function of y for all $t > 0$. Suppose the initial particle velocity is unique, i.e., $v_0(y_0)$ is a single-valued function of y_0. For $v(y,t)$ to become a multi-valued function of y, $\partial v/\partial y$ must become infinite at some y and t. Provided $\partial v/\partial y$ remains finite for all y and t, single-valuedness (or uniqueness) of the particle velocity field is guaranteed. Since, from Eq. (19)

$$\frac{\partial v}{\partial y} = \frac{\mathrm{d}v_0}{\mathrm{d}y_0}\left(\frac{\partial y}{\partial y_0}\right)^{-1} e^{-t/\tau}, \tag{21}$$

the condition for single-valuedness becomes $\partial y/\partial y_0 > 0$. From Eq. (20),

$$\frac{\partial y}{\partial y_0} = 1 + \frac{\mathrm{d}v_0}{\mathrm{d}y_0}\tau(1 - e^{-t/\tau}), \tag{22}$$

based on which Meiburg et al. (1999) obtained the condition for unique particle velocity field to be

$$-1 < \frac{\mathrm{d}v_0}{\mathrm{d}y_0}\tau. \tag{23}$$

If the above condition is violated, then a multi-valued particle velocity field will develop in finite time. To deal with such fields, one needs to consider the particle distribution function, $f(\mathbf{x}, \mathbf{v}, t)$ in phase space, whose evolution is controlled by a Boltzmann-like equation (Williams, 1985; Meiburg et al., 1999).

The above condition is very similar to the more general condition derived in the previous section. However, certain distinctions are warranted. Both the conditions (Eq. (23) and $-1 < \sigma_2\tau$) guarantee that an initially single-valued particle velocity field will remain single-valued at all later times. For the case considered in Section 2.2 a multi-valued $\mathbf{v}$ can arise only when $|\nabla\mathbf{v}| \to \infty$; in other words a multi-valued $\mathbf{v}$ entails $\sigma_{\min} \to -\infty$. The condition $-1 < \sigma_2\tau$ automatically sets a finite lower bound on $\sigma_{\min}$, thus guaranteeing a single-valued particle velocity field. In case of particles falling in still air Meiburg et al. (1999) show that it suffices to set a bound on the *initial* velocity gradient. In the more general case, however, a bound on the initial particle velocity field

alone will not guarantee single-valuedness, owing to the possibility of a complex underlying fluid velocity field.

Our result is about the asymptotic behavior of multi-valued particle fields (i.e., functions $f(\mathbf{x},\mathbf{v},t)$ which are non-zero at multiple values of $\mathbf{v}$ for at least some $\mathbf{x}$). In the case of particles settling in still air, their asymptotic behavior is quite simple: all particles approach their unique terminal velocity exponentially fast, irrespective of the initial particle distribution, $f(\mathbf{x},\mathbf{v},t=0)$. The analysis of Section 2.2 implies that even in the presence of complex fluid motion, provided $\sigma_{\min}\tau$ remains greater than -1 throughout a region of fluid over a range of time (in other words if $-1<\sigma_2\tau$), the particle velocity field estimated from Eq. (B.1) may be regarded as unique. We will refer to such a field as an *equilibrium* particle velocity field, implying that it is asymptotically valid after the decay of initial transients. Since a particle velocity field can depend only on initial conditions and fluid quantities, an equilibrium field is determined solely by fluid quantities. In particular, $\sigma_{\min}$ is determined by fluid quantities, which means that particle velocity fields remain in equilibrium provided the fluid field is sufficiently well behaved. The equilibrium particle velocity differs from the fluid velocity only at $O(\tau)$ and therefore, to leading order, the condition for equilibrium particle velocity can be approximately stated as $-1<\sigma_u\tau$, where σ_u is the minimal eigenvalue of the strain-rate tensor of the fluid velocity field. However, during the initial transient the particle velocity field can differ arbitrarily from the background fluid velocity, and therefore the approach to equilibrium can be guaranteed only by $-1<\sigma_{\min}\tau$.

Three things can disrupt a particle field from approaching its equilibrium velocity. First, $\sigma_{\min}\tau$ can become less than -1. When this happens the stable equilibrium velocity field becomes unstable, and the particles' velocities begin to diverge exponentially from it. Second, particles can collide with boundaries. In this case, particles suffer a sudden change in their velocities, when they bounce off the surface. Depending on the nature (specular or diffuse) of reflection, the particle distribution function $f(\mathbf{x},\mathbf{v},t)$ can have a dominant bimodal or dispersed character in $\mathbf{v}$. This non-uniqueness in particle velocity is likely to dominate in the near-wall region, and particles then need to re-adjust to the equilibrium velocity away from the boundaries. This situation is clearly complicated by the change of the governing equation for particle motion in the presence of a boundary, which, of course, is not represented in Eq. (B.1). Third, particles can collide with each other. The notion of an equilibrium velocity is still useful: particles will return to equilibrium provided the particle volume fraction is not so high that the mean time between collisions is less than the particle response time. Again inter-particle collision is not accounted for in Eq. (B.1).

With the above caveats, particle velocities are unique for small τ. This significantly simplifies the concept of an Eulerian method. It eliminates the need for averaging over an ensemble of particle velocities. Nevertheless, the existence of a unique velocity field does not imply that the expansion in Eq. (16) is accurate. To assess its accuracy we turn to numerics.

3. Numerical results

3.1. Description of the DNS

Direct numerical simulation (DNS) of a turbulent channel flow is performed in a channel with dimensions $4\pi h$ in the streamwise (x), $2h$ in the wall-normal (y), and $4\pi h/3$ in the spanwise (z)

direction. The Reynolds number based on half channel height and friction velocity is $Re_\tau = 180$. The DNS employs a fully de-aliased, pseudospectral algorithm on a grid of size $128 \times 128 \times 128$. The time-step in wall units is $\Delta t^+ = 0.054$.

Motion of individual particles is governed by

$$\frac{\mathrm{d}\boldsymbol{\xi}^+}{\mathrm{d}t^+} = \mathbf{v}^+, \quad \frac{\mathrm{d}\mathbf{v}^+}{\mathrm{d}t^+} = \frac{1}{\tau^+}\left(\mathbf{u}^+(\boldsymbol{\xi}^+, t^+) - \mathbf{v}^+\right) + \beta\frac{\mathrm{D}\mathbf{u}^+}{\mathrm{D}t^+}, \tag{24}$$

where the superscript '+' indicates a non-dimensional variable in wall units.

In the simulation, the only forces influencing particle motion are Stokes drag and added mass. Finite Reynolds number effects on particle drag are ignored. The particles neither modify the fluid flow nor interact with each other. They rebound purely elastically if their centers come in contact with the wall.

Eighteen types of particles are considered in this study: nine dense particles ($\beta = 0$) and nine bubbles ($\beta = 3$). In each case, the particle response times are chosen to be powers of $10^{1/4}$ ranging from $10^{-6/4}$ to $10^{2/4}$ (i.e., $\tau^+ = 0.03, 0.06, 0.1, 0.2, 0.3, 0.6, 1.0, 1.8, 3.2$). 300,000 particles of each type are used. Particle statistics are obtained as a function of the inhomogeneous, wall-normal direction, with averaging along the streamwise and spanwise directions. The large number of particles allows for reasonably converged statistics to be obtained as a function of the wall-normal direction.

The lower limit of $\tau^+ = 0.03$ was chosen because Eq. (24) becomes too stiff for lower τ^+. There are methods that overcome this stiffness (Ling et al., 1998), but they are too analogous to using an explicit expression for $\mathbf{v}$ to serve as a useful tool for comparison.

3.2. Static results

The particles are given initial velocities equal to the fluid's. Particles are advanced in time for 54 wall units, which is 17 times the response time of the largest particle. At this point it may be regarded that all particles have adjusted to the flow. We compare the actual particle velocities (obtained by following particles using the Lagrangian equation of motion, Eq. (24)) to those

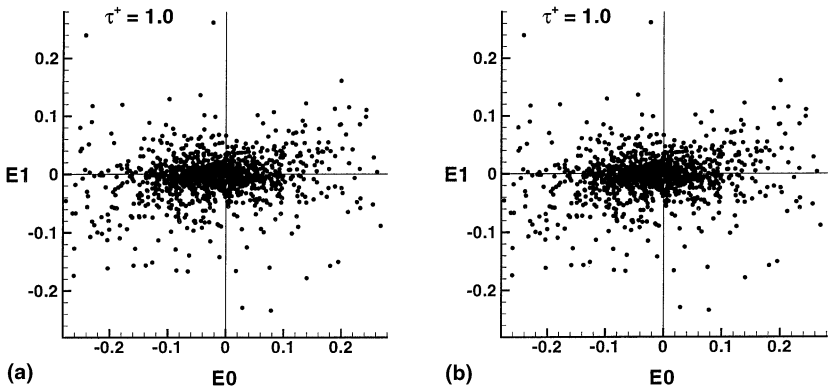

Fig. 3. Zeroth- vs. first-order errors for large $\tau^+(\beta = 0, y^+ = 20)$: (a) streamwise components; (b) wall-normal components.

predicted by Eq. (16). We define E0, E1, and E2 to be errors resulting from a zeroth, first-, and second-order Eulerian approximation, respectively, i.e.,

$$\mathrm{E0} = \mathbf{u}^+ - \mathbf{v}^+, \tag{25}$$

$$\mathrm{E1} = \left(\mathbf{u}^+ - (1-\beta)\frac{\mathrm{D}\mathbf{u}^+}{\mathrm{D}t^+}\tau^+\right) - \mathbf{v}^+, \tag{26}$$

$$\mathrm{E2} = \left(\mathbf{u}^+ - (1-\beta)\left(\frac{\mathrm{D}\mathbf{u}^+}{\mathrm{D}t^+}\tau^+ - \left(\frac{\mathrm{D}^2\mathbf{u}^+}{\mathrm{D}t^{+2}} + \frac{\mathrm{D}\mathbf{u}^+}{\mathrm{D}t^+}\cdot\nabla\mathbf{u}^+\right)\tau^{+2}\right)\right) - \mathbf{v}^+. \tag{27}$$

The zeroth-order error, E0, is the error in approximating the particle velocity to be simply the local fluid velocity. We expect the first-order correction in τ^+ to bring about significant improvement for small particles, which should appear as measurable reduction in the first-order error, E1 compared to E0. We also pursue one more term in the expansion to investigate its ability to predict particle velocity more accurately.

Fig. 3 compares E1 to E0 for the third-largest particle type ($\tau^+ = 1$), for the dense-particle case ($\beta = 0$). Fig. 3(a) shows a scatter plot of the streamwise component of E1 versus that of E0 for all particles within a narrow horizontal layer of fluid in the neighborhood of $y^+ = 20$. Fig. 3(b) shows the corresponding scatter plot for the wall-normal component. Two observations can be made from these plots. First, the E1 errors are smaller on average than E0 errors. Although the difference does not appear to be appreciable, the first-order correction does seem to make a positive contribution to accurate prediction of particle velocity. Second, while the first-order error, E1, appears to be evenly distributed with equal contribution from both positive and negative errors, the zeroth-order error, E0 exhibits a bias. The bias is negative for the streamwise component and positive for wall-normal component, the bias being more apparent in the latter case. This suggests that the first-order approximation better captures the average behavior of the particle motion in both the streamwise and wall-normal directions. On the other hand, E0, by approximating the particle velocity to be the same as local fluid velocity, ignores the tendency of the particles to lead

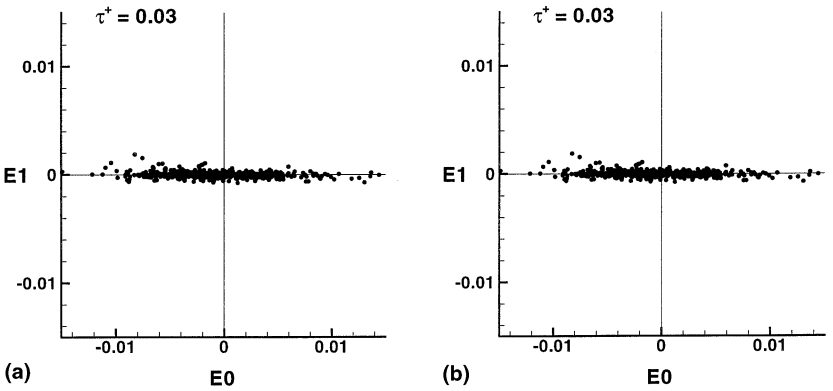

Fig. 4. Zeroth- vs. first-order errors for small $\tau^+(\beta = 0, y^+ = 20)$: (a) streamwise components; (b) wall-normal components.

the fluid in their streamwise motion close to the wall. In the wall-normal direction, the zeroth-order approximation similarly ignores the wallward migration of particles.

Fig. 4 makes the same comparisons as Fig. 3, but for the smallest particle type ($\tau^+ = 0.03$). The same features are evident, but the first-order errors are now much smaller than the zeroth-order errors. A closer look at the scatter plots reveals that the bias observed in Fig. 3 for the zeroth-order error persists for the smaller particles as well, although the magnitude of this bias is somewhat diminished. Scatter plots for other values of τ^+, at other y^+ locations, and for bubbles ($\beta = 3$) are similar. From these scatter plots mean and root mean square (rms) errors can be computed for $E0$ and $E1$. The results on mean and rms errors for the different particle types will be shown below.

Fig. 5 shows the rms values of $E0, E1$, and $E2$ as a function of τ^+ for the dense particles ($\beta = 0$) in the buffer region at $y^+ = 20$. As expected, the $E1$ errors decrease with τ^+ more rapidly than the $E0$ errors. The $E2$ errors fall off still more rapidly, but become smaller than $E1$ only for very small particles ($\tau^+ < 0.1$). The behavior is similar for both the streamwise (Fig. 5(a)) and wall-normal (Fig. 5(b)) components. The fact that the $E2$ errors are large than the $E1$ errors for larger particles suggests one of two things. The power series for $\mathbf{v}$ may not be convergent for particles of larger time constant. Or it may be that in the computation of $E2$ the requisite second derivatives both in time and space are too sensitive for accurate numerical evaluation. In either case, the extra work involved in using the second-order approximation is not worth even the paltry improvement for small τ^+, let alone the worse results for large τ^+.

Fig. 6 shows the average values of $E0, E1$, and $E2$ at $y^+ = 20$. The first-order approximation captures well the mean particle motion, while the zeroth-order approximation leads to significant misprediction of the mean motion of the particles. In the buffer region at $y^+ = 20$ the particles lead the fluid, and therefore approximating the particle velocity to be the same as the local fluid velocity underestimates the mean streamwise motion of the particles. The underestimation increases with τ^+. In the case of wall-normal motion, particles tend to migrate toward the walls due to turbophoresis (Reeks, 1983), thus in the bottom half of the channel the mean particle wall-normal velocity is negative. Since the mean wall-normal velocity of the fluid is zero due to continuity, the zeroth-order approximation ($E0$) results in significant positive error. The corresponding error in

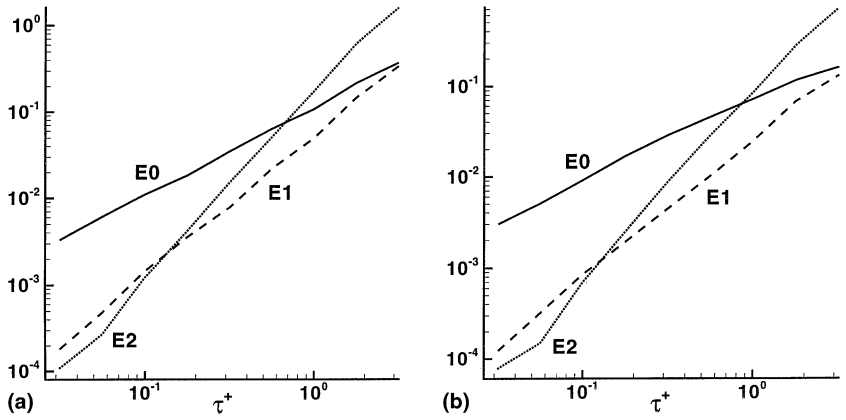

Fig. 5. Root mean square errors for $\beta = 0$ particles at $y^+ = 20$: (a) streamwise errors; (b) wall-normal errors.

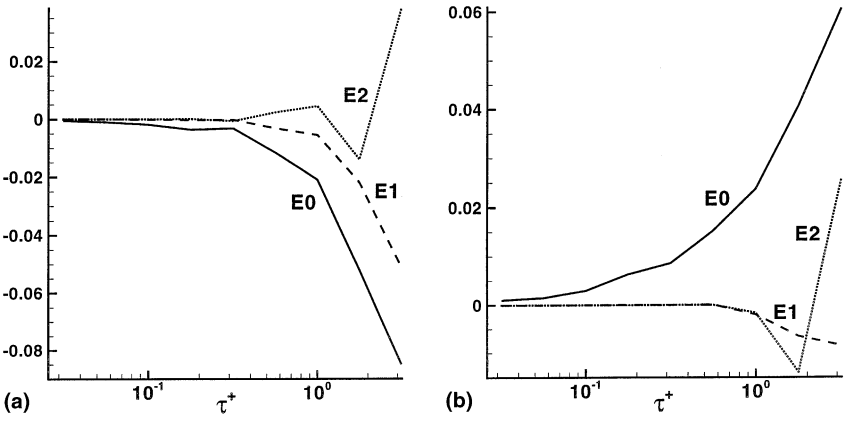

Fig. 6. Mean errors for $\beta = 0$ particles at $y^+ = 20$: (a) streamwise errors; (b) wall-normal errors.

the upper half of the channel will be negative. It is worth nothing that for $\tau^+ < 0.4$ the mean error in both streamwise and wall-normal components is nearly zero for the first- and second-order approximations. In both the streamwise and the wall-normal components, the ratio of the average $E1$ error to the average $E0$ error is smaller than the ratio of the rms $E1$ error to the rms $E0$ error for all τ^+. Likewise, the second-order approximation has a much better average behavior than rms behavior. Because the average behavior is better than the rms behavior, we might hope that using the first-order approximation for $\mathbf{v}$ will produce better results than using the zeroth-order approximation, even for $\tau^+ = 3$, despite the fact that the rms $E0$ and $E1$ errors have the same magnitude. This will be explored in Section 3.3.

Fig. 7 shows streamwise rms values of $E0, E1$, and $E2$ at the channel midplane ($y^+ = 180$) and in the near-wall region ($y^+ = 2$). At $y^+ = 180$ the $E1$ error is relatively small at $\tau^+ = 3$, but the $E2$ error is extremely large. At $y^+ = 2$, both the $E1$ and $E2$ errors behave well. The most important result, that the first-order approximation is a significant improvement over the zeroth-order approximation, holds throughout the channel. Similar observations can be made about the behavior

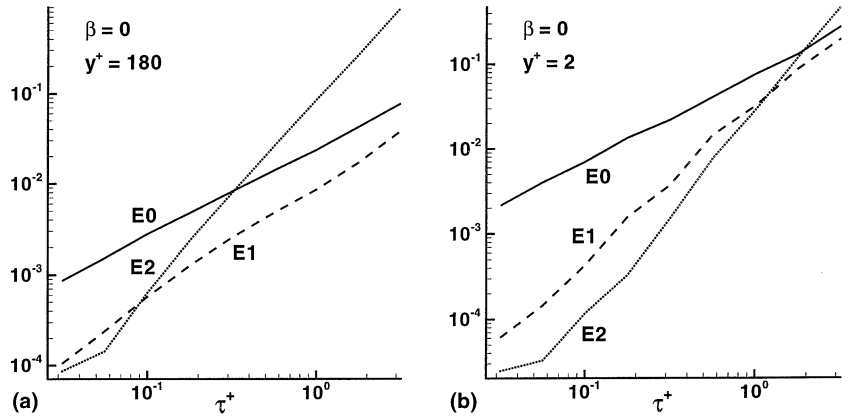

Fig. 7. Streamwise rms errors for $\beta = 0$ particles at other y^+: (a) near the midplane; (b) near the wall.

of the mean errors (not shown here). Fig. 8 shows the rms error for the bubble case ($\beta = 3$). The plots are quite similar to those in Fig. 5. In general, there is no significant qualitative difference between the $\beta = 0$ and $\beta = 3$ cases, though the mean error plots are of opposite sign since the mean behavior of bubbles is opposite to that of dense particles.

3.3. Dynamic results

Section 3.2 compared the actual velocities of particles (computed by the Lagrangian method) with the velocities obtained by several approximations to the Eulerial field $\mathbf{v}(\mathbf{x}, t)$. The comparison was performed at an instant in time so as to assess the accuracy of the Eulerian approximation at various orders. Although the errors are generally small for the first- and higher-order approximations, it needs to be determined whether the errors will accumulate over time, eventually giving rise to large errors. If we compare the path of an individual particle evolved using the actual Lagrangian velocity with that of an identical particle (with an identical initial condition) using an approximate Eulerian velocity, then these paths will always diverge in a turbulent flow. Small differences in the particle velocity are guaranteed to make the paths diverge exponentially fast. In fact, even with the Lagrangian approach the particle paths will diverge if two different interpolation or integration schemes are used (Balachandar and Maxey, 1989). But it is not the history of individual particles that is of interest in an Eulerian method. Therefore, it is more meaningful to look at whether particles evolved using an approximate Eulerian velocity exhibit the same statistical behavior as particles evolved using the exact velocity. Druzhinin and Elghobashi (1998) performed a similar experiment in the context of micro-bubbles in a Taylor–Green vortex. The Eulerian approximation was observed to give accurate predictions of bubble concentration over short times, but over long times there was a slowly growing disparity between the two approaches. However, this accumulation of error may be due to the steady, laminar nature of the Taylor–Green vortex.

In a turbulent flow it may be expected that the errors do not accumulate so dramatically. Errors are likely to build up only as long as a particle stays correlated with an eddy, after which the particle sees new flow conditions. For example, in the limit of the zeroth-order approximation the

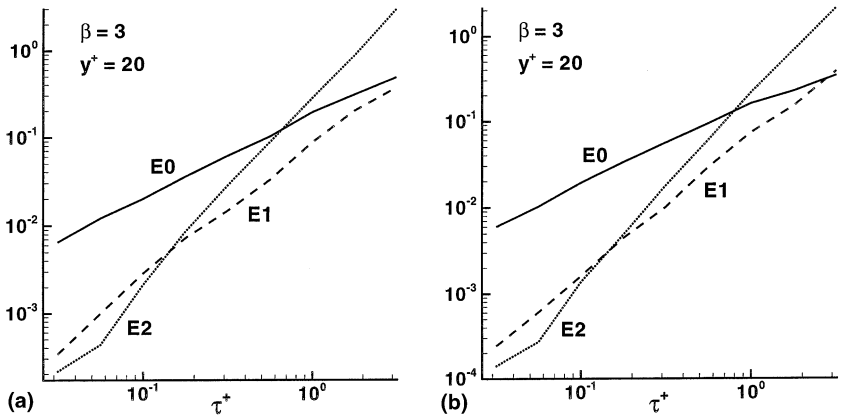

Fig. 8. Root mean square errors for $\beta = 3$ particles (bubbles) at $y^+ = 20$: (a) streamwise errors; (b) wall-normal errors.

long-time asymptotic error is simply the difference between particle and fluid statistics (provided particles stay uniformly distributed). Yeung and Pope (1989), Squires and Eaton (1991) and Elghobashi and Truesdell (1992) have examined the difference between true particle (Lagrangian) and fluid statistics in isotropic turbulence. The error in higher-order Eulerian approximations will be bounded by this difference. Thus there is reason to believe that at all orders of Eulerian approximation to particle velocity, any error in statistics will quickly reach its asymptotic value on an eddy-particle correlation time-scale.

The results of Section 3.2 were evaluated at the time-instant $t^+ = 54$. In order to evaluate the ability of the Eulerian approximation to track particle statistics accurately over time, two sets of statistics were obtained by integrating the particle motion further for another 1000 wall units. The first set of particles were evolved in time using the exact particle velocity given by Eq. (24). The statistics obtained from this set will be termed *exact*. The second set of particles, whose initial positions coincide with those of the first set, were evolved using the first-order Eulerian approximation $\mathbf{v}^+ = \mathbf{u}^+ - (1-\beta)\tau^+ \mathrm{D}\mathbf{u}^+/\mathrm{D}t^+$. Statistics obtained from this set of particles will be termed *approximate*. Where appropriate, corresponding fluid statistics averaged over the fluid volume will also be provided – these would be the zeroth-order approximation to particle statistics as well. For each type of particle (specified by a value of β and of τ^+) we form averages and probability density functions (PDFs) based on an ensemble consisting of all particles within some thin horizontal slab of fluid (e.g., near $y^+ = 20$) over a time interval of 380 wall units. We use the notation $\langle q \rangle (y^+)$ to denote the average of the quantity q over all particles within the thin horizontal slab of fluid centered around y^+. All the statistics on the discrepancies between the exact and approximate methods have converged: they are essentially the same at other time-instants as well.

The first quantity we examine is $\mathrm{Tr}(\mathbf{G}^{+2})$, where $\mathbf{G}^+ = \nabla\mathbf{u}^+$. This quantity can also be expressed as $u^+_{i,j}u^+_{j,i}$, or $|\mathbf{S}^+|^2 - |\Omega^+|^2$, the difference between the magnitudes of the strain and rotational components of the gradient tensor. Using an expansion like that in Eq. (16), Maxey (1987) showed that dense particles tend to congregate where $\mathrm{Tr}(\mathbf{G}^{+2})$ is large, and bubbles tend to congregate where $\mathrm{Tr}(\mathbf{G}^{+2})$ is small. Zhou et al. (1998) extended this idea to get an approximate formula for the particle number density as a function of $\mathrm{Tr}(\mathbf{G}^{+2})$. Thus $\mathrm{Tr}(\mathbf{G}^{+2})$ is a good quantity to characterize preferential accumulation of particles and bubbles. Fig. 9 compares the average

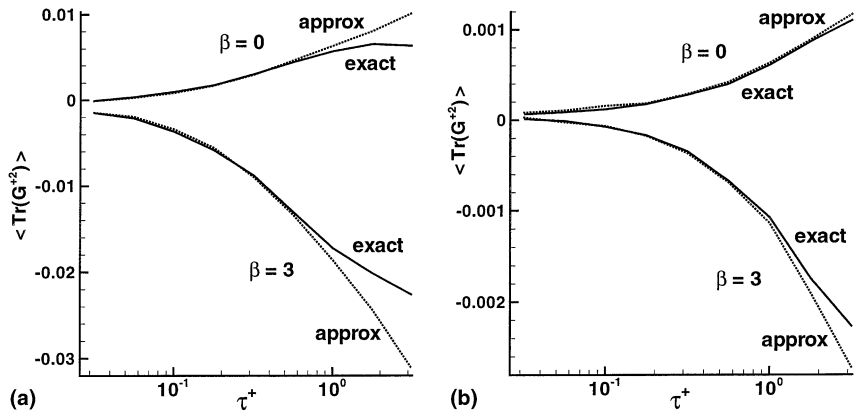

Fig. 9. Mean values of $\mathrm{Tr}(\mathbf{G}^{+2})$: (a) at $y^+ = 20$; (b) at $y^+ = 180$.

value of $\mathrm{Tr}(\mathbf{G}^{+2})$ for "exact" and "approximate" particles in the buffer region ($y^+ = 20$) and at the channel midplane ($y^+ = 180$). The preferential accumulation of dense particles ($\beta = 0$) in regions of strain, and bubbles ($\beta = 3$) in regions of vorticity, is clearly evident in the respective positive and negative mean values of $\mathrm{Tr}(\mathbf{G}^{+2})$. The discrepancy between exact and approximate statistics is significant in the buffer region only for $\tau^+ > 1$. Near the channel midplane the first-order Eulerian approximation appears to be accurate even for the largest particle and bubble types considered ($\tau^+ = 3$). The PDFs of $\mathrm{Tr}(\mathbf{G}^{+2})$ at $y^+ = 20$ for $\tau^+ = 3$ are shown in Fig. 10. By comparing the exact and the first-order approximate PDFs to the PDF for the fluid, we see clearly the preference of dense particles for positive $\mathrm{Tr}(\mathbf{G}^{+2})$, and of bubbles for negative $\mathrm{Tr}(\mathbf{G}^{+2})$. Despite the relatively large departures seen in Fig. 9, the PDFs of the exact and approximate particles do not disagree much qualitatively even for this worst-case scenario ($y^+ = 20, \tau^+ = 3$). They agree with each other much more closely than they do with the PDF for the fluid. This indicates that the dynamic behavior of the approximation is much better than the static behavior: Figs. 5 and 8 suggest that for $\tau^+ = 3$ the first-order approximation to particle velocity is just as bad as zeroth-order approximation. While this is true at an instant in time, Fig. 10 indicates that the first-order approximation accounts for preferential accumulation of particles and bubbles to sufficient accuracy, resulting in an accurate representation of the conditional statistics with respect to $\mathrm{Tr}(\mathbf{G}^{+2})$. For the less extreme cases (i.e., smaller τ^+), the exact and approximate particle PDFs are virtually identical.

One might argue that the behavior for $\mathrm{Tr}(\mathbf{G}^{+2})$ is somehow built in, since taking the divergence of the approximate particle velocity $\mathbf{v}^+ = \mathbf{u}^+ - (1-\beta)\tau^+ \mathrm{D}\mathbf{u}^+/\mathrm{D}t^+$ yields $\nabla \cdot \mathbf{v}^+ = -(1-\beta)\tau^+ \mathrm{Tr}(\mathbf{G}^{+2})$. Indeed, with $\beta = 0$, this is the equation that Maxey (1987) used to argue that $\mathrm{Tr}(\mathbf{G}^{+2})$ determines the preferential concentration of particles. Zhou et al. (1996, 1999) have defined local *swirling strength*, λ_i^+, to be a good discriminator for identifying vortices. Swirling strength is defined as the magnitude of imaginary part of the complex conjugate eigenvalues of $\nabla \mathbf{u}^+$ (swirling strength is 0 if all the eigenvalues are real). Ferry and Balachandar (1999) have shown that λ_i^+ is a more sensitive predictor of particle concentration than $\mathrm{Tr}(\mathbf{G}^{+2})$ is. Fig. 11 compares exact and approximate statistics using λ_i^+ instead of $\mathrm{Tr}(\mathbf{G}^{+2})$, and the plots indicate the same thing as the plots of $\mathrm{Tr}(\mathbf{G}^{+2})$. There is a discrepancy only for the largest response time considered ($\tau^+ = 3$).

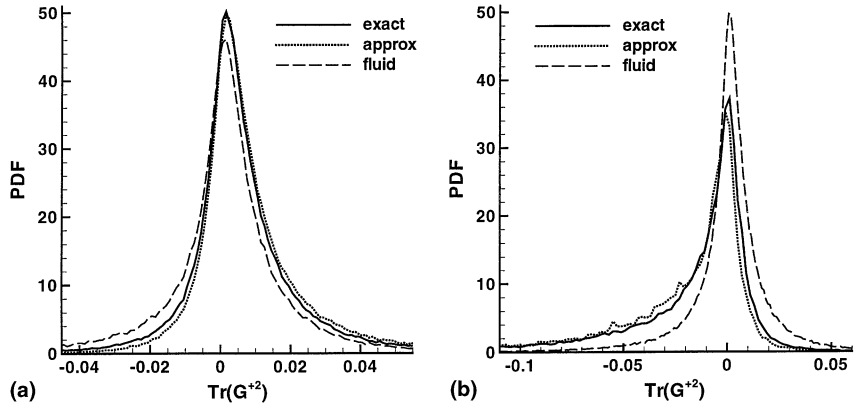

Fig. 10. PDFs of $\mathrm{Tr}(\mathbf{G}^{+2})$ for $\tau^+ = 3$ at $y^+ = 20$: (a) for $\beta = 0$; (b) for $\beta = 3$.

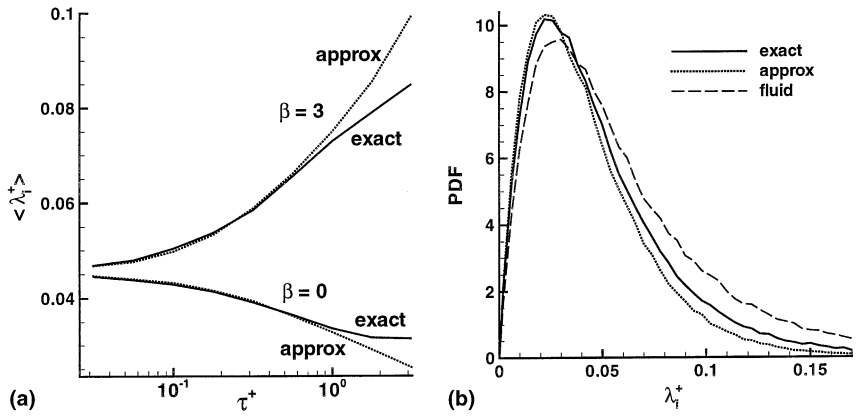

Fig. 11. Plots of swirling strength at $y^+ = 20$: (a) mean values; (b) PDFs for $\beta = 0$, $\tau^+ = 3$.

The first-order approximation tends to overpredict the preferential concentration of both the particles and the bubbles. Nevertheless, even for the largest τ^+ the PDFs look qualitatively similar (see Fig. 11(b)) when compared to the PDF of the fluid. The discrepancy in $\langle \lambda_i^+ \rangle$ is due to the first-order approximation's exaggeration of the abhorrence of particles toward regions of large λ_i^+. However, the agreement of the PDFs is surprisingly good especially when compared to the static result for $\tau^+ = 3$ presented in Fig. 5.

Fig. 12 examines the statistics $u_1^+ - v_1^+$, the streamwise relative velocity between fluid and particle. For the larger particles and bubbles there is a tendency for the first-order approximation to underestimate the relative velocity. To leading order, the relative velocity can be expressed in terms of local fluid velocity derivative as $(1 - \beta)\tau^+ \mathrm{D}\mathbf{u}^+/\mathrm{D}t^+$. The mean streamwise relative velocity is primarily induced by turbophoresis, and the local fluid velocity derivatives are unable to fully account for the net flux of particles from adjacent faster- or slower-moving layers. Note that the one case that does not exhibit much error is that of dense particles ($\beta = 0$) near the channel midplane ($y^+ = 180$), where there is no net flux of particles on average. Figs. 13 and 14 show

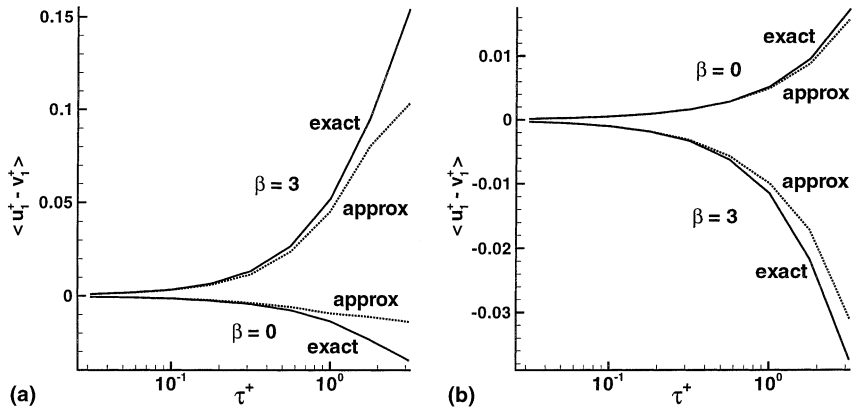

Fig. 12. Mean values of $u_1^+ - v_1^+$: (a) at $y^+ = 20$; (b) at $y^+ = 180$.

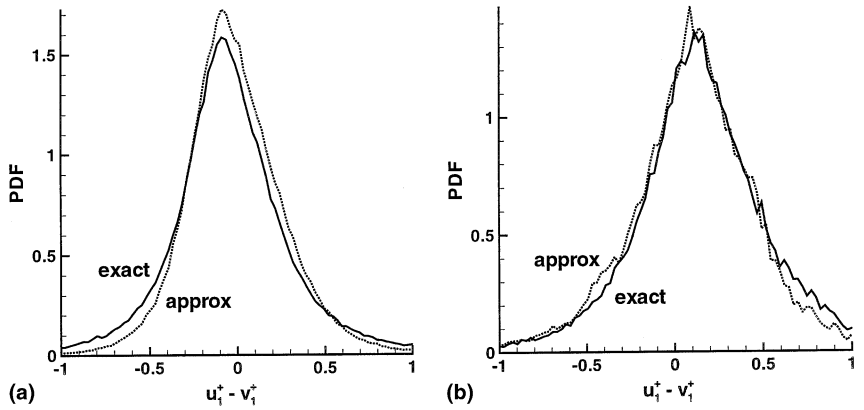

Fig. 13. PDFs of $u_1^+ - v_1^+$ for $\tau^+ = 3$ at $y^+ = 20$: (a) for $\beta = 0$; (b) for $\beta = 3$.

PDFs of $u_1^+ - v_1^+$ for both the dense particles and bubbles. In Fig. 13(a) it is clear that the underprediction of streamwise relative velocity is due to the stronger peak in the PDF corresponding to zero relative velocity and the corresponding under-representation of particles moving faster than the local flow. The agreement between the PDFs at the channel midplane in Fig. 14 is good.

The statistics of $u_2^+ - v_2^+$, the wall-normal relative velocity, in the buffer region is shown in Fig. 15. Here the trend is somewhat opposite to that observed in Fig. 12(a): the average wall-normal relative velocity based on the first-order approximation exceeds the exact value. Nevertheless, the corresponding PDFs for the largest particle type in Fig. 16 show good agreement. In comparison, the PDF of the zeroth-order Eulerian approximation is a Dirac delta function corresponding to identically zero relative velocity. Given this extreme, the inclusion of the first-order correction can be seen to bring significant improvement. The cumulative effect of wall-normal migration can be felt in particle number density. Fig. 15(b) shows the normalized number density of dense particles and bubbles at $y^+ = 20$ as a function of particle response time. Here normalization is with respect to the initial uniform distribution of particles across the channel. An increase in the concentration

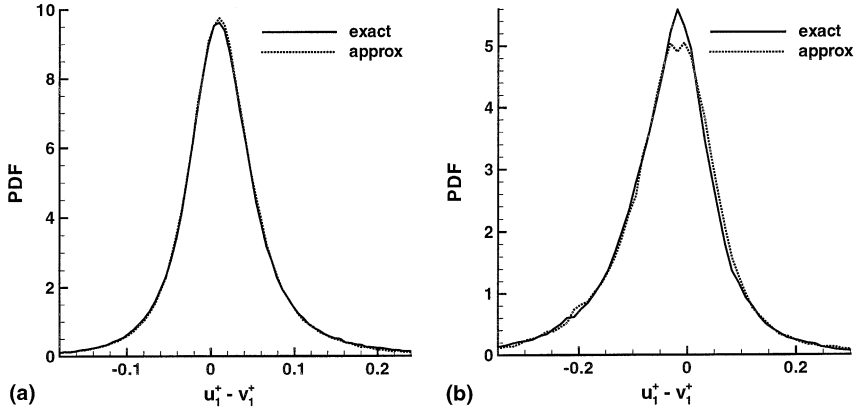

Fig. 14. PDFs of $u_1^+ - v_1^+$ for $\tau^+ = 3$ at $y^+ = 180$: (a) for $\beta = 0$; (b) for $\beta = 3$.

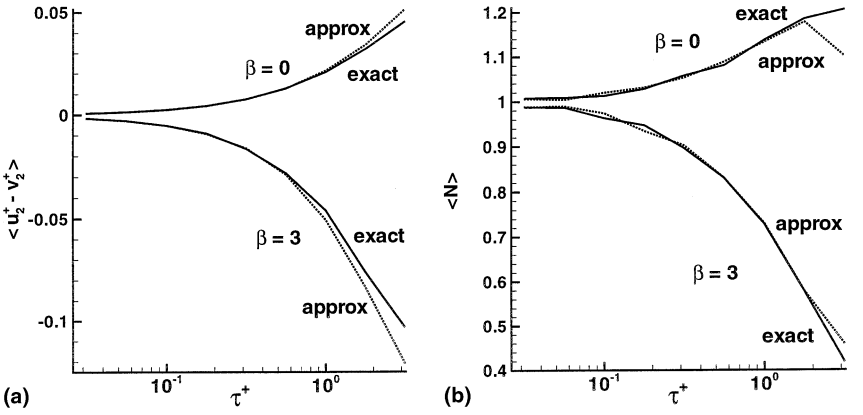

Fig. 15. Mean wallward motion statistics at $y^+ = 20$: (a) mean of $u_2^+ - v_2^+$; (b) normalized number density.

of particles and a strong depletion of bubbles in the buffer region are evident. It is also clear that the first-order Eulerian approximation captures this wall-normal migration of particles and bubbles quite well.

Finally we will address the question of how well particles of different sizes satisfy the condition for uniqueness obtained in Section 2.2 in the present case of turbulent channel flow. In Section 2.2 the condition for uniqueness is expressed in terms of $\sigma_{\min}$, the minimal eigenvalue of $\frac{1}{2}(\nabla\mathbf{v} + (\nabla\mathbf{v})^{\mathrm{T}})$. Since the exact particle velocity field $\mathbf{v}(\mathbf{x}, t)$ is not known, we will instead consider σ_u, the minimal eigenvalue of $\frac{1}{2}(\nabla\mathbf{u} + (\nabla\mathbf{u})^{\mathrm{T}})$. It follows from Eq. (16) that $\sigma_{\min} = \sigma_u + \mathrm{O}(\tau)$, so we obtain only approximate information about uniqueness. The average of σ_u, measured in wall units, for particles in the buffer region ($y^+ = 20$) is presented in Fig. 17. Since the bubbles prefer regions of low strain, and the particles prefer high strain, it is no surprise that bubble statistics yield a smaller value of $|\langle\sigma_u^+\rangle|$ than the fluid, and the particle statistics yield a larger value. The criterion for uniqueness can be approximately stated as $-1 < \tau^+\sigma_u^+$. Thus, as far as the mean value

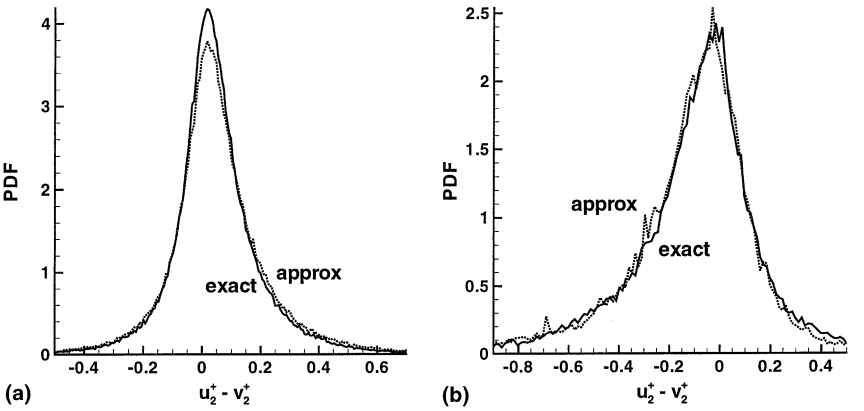

Fig. 16. PDFs of $u_2^+ - v_2^+$ for $\tau^+ = 3$ at $y^+ = 20$: (a) for $\beta = 0$; (b) for $\beta = 3$.

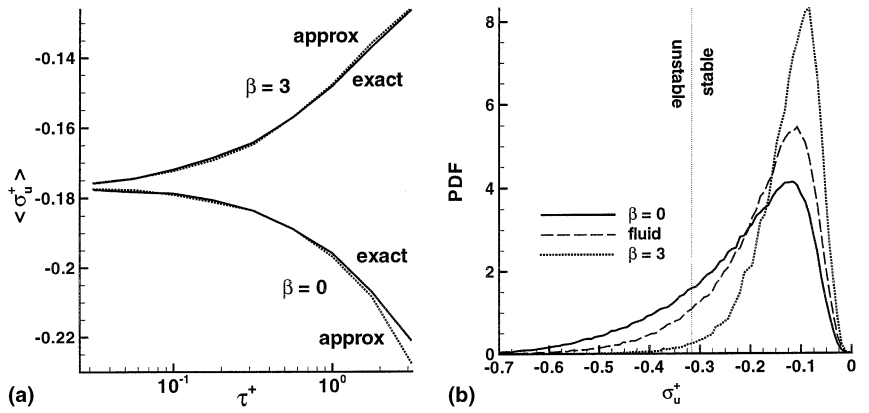

Fig. 17. σ_u^+ at $y^+ = 20$: (a) mean; (b) PDF for $\tau^+ = 3$.

of σ_u^+ is concerned, all particle and bubble types satisfy the condition for unique particle velocity field.

We do expect the criterion for uniqueness to be violated at least some of the time as the particles and bubbles get larger. Fig. 17(b) shows the PDF of σ_u^+ for the largest particle and bubble types ($\tau^+ = 3$). Also shown is the corresponding fluid PDF, which exhibits an intermediate behavior. The preference of particles for high strain regions is reflected in the smaller peak and the long negative tail. As a result, during a significant fraction of their trajectories dense particles experience a compressive strain of magnitude greater than 1/3. This would suggest that a unique particle velocity field is not quite appropriate for dense particles of $\tau^+ = 3$. On the other hand, bubbles avoid regions of high strain, resulting in a sharply peaked PDF with a weak negative tail. The criterion for uniqueness therefore seems to be reasonably well satisfied for the case of bubbles of $\tau^+ = 3$. The PDFs do not vary dramatically as τ^+ is varied, either for the dense particles or the bubbles: as τ^+ is decreased, the PDFs approach the fluid PDF. So it can be inferred that a unique velocity field is well justified for dense particles of $\tau^+ \lesssim 1/0.7$ and for bubbles of $\tau^+ \lesssim 1/0.4$. The

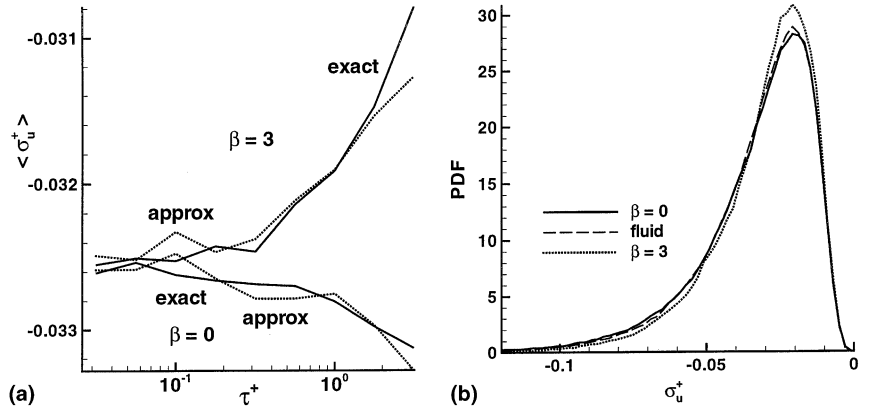

Fig. 18. σ_u^+ at $y^+ = 180$: (a) mean; (b) PDF for $\tau^+ = 3$.

corresponding $\langle \sigma_u^+ \rangle$ and PDFs at the channel midplane are given in Fig. 18. As could be expected the compressive strain has a smaller magnitude at the channel midplane, and a unique velocity field appears to be justified for both dense particles and bubbles of $\tau^+ \lesssim 8$.

The results of this section justify the use of the fast Eularian method for small τ. Although the comparisons are performed on a dataset of particles evolved by the Lagrangian method, this is equivalent to sampling data at a certain set of positions from an Eulerian method (or, more precisely, from a generalized Eulerian method that evolves not just a single velocity field, but rather a velocity distribution field $f(\mathbf{x}, \mathbf{v}, t)$). In the limit of an infinite ensemble of particles, there would be no distinction between statistics gathered by Lagrangian and Eulerian methods. Therefore, sampling at a finite number of particle positions can only exaggerate the difference between the standard and fast Eulerian methods.

4. Physical consequences

4.1. Particle distribution

The numerical results suggest that the first- (and higher-) order terms in the Eulerian approximation to particle velocity do not just improve the accuracy of prediction (over the zeroth-order), but incorporate important physics, such as preferential accumulation and turbophoresis, which are otherwise left unaccounted for.

From Eq. (16) the divergence of the particle velocity field can be expressed as

$$\nabla \cdot \mathbf{v} = -(1-\beta)\mathrm{Tr}(\mathbf{G}^2)\tau + \mathrm{O}(\tau^2), \tag{28}$$

provided $\nabla \cdot \mathbf{g} = 0$. As seen earlier, the leading-order term accounts for the preferential accumulation of dense particles in regions of high strain and bubbles in regions of high vorticity. Simply approximating the particle velocity as equal to the local fluid velocity completely ignores the preferential accumulation of particles and bubbles and the important subsequent effects arising from this behavior. Figs. 9 and 10 show that the method captures this preferential accumulation in practice as well as theory.

Fig. 6 shows that the first-order term in the Eulerian approximation of $\mathbf{v}$ captures the average wallward motion quite well. Again, this is predicted by theory: if Eq. (16) is averaged over horizontal planes, then, assuming $\nabla \cdot \mathbf{g}$ and g_2 are zero, we find

$$\overline{v_2} = (1-\beta)\left(\left(-\frac{\partial}{\partial y}\overline{u_2^2}\right)\tau + \left(2\frac{\partial^2}{\partial t \partial y}\overline{u_2^2} + \frac{\partial^2}{\partial y^2}\overline{u_2^3} - \overline{u_2 \mathrm{Tr}(\mathbf{G}^2)}\right)\tau^2\right) + \mathrm{O}(\tau^3), \tag{29}$$

where we make use of the fact that $\overline{u_2} = 0$ and the horizontal directions are periodic. In the above, the notation $\bar{q}$ means an average over the $x-z$ plane, which is different from the previously defined $\langle q \rangle$. $\langle q \rangle$ is the average over all the particles on a horizontal plane and therefore may be thought of as a Favre average: $\langle q \rangle = \overline{cq}/\bar{c}$, where the concentration c is the weighting that accounts for the preferential distribution of particles over the plane.

Clearly at the zeroth-order approximation there is no inertial migration of particles or bubbles toward or away from the walls. The $\mathrm{O}(\tau)$ approximation of $\bar{v}_2$ gives the same expression for the turbophoretic velocity as obtained by Camparaloni et al. (1975) and Reeks (1983). At this level of

approximation it is the wall-normal gradient in the rms wall-normal turbulent fluctuating fluid velocity that drives the inertial migration – so the effect is termed turbophoresis. The above equation allows for the identification of higher-order effects as well. The second-order correction is due to: (a) the time-rate of change of the first-order term; (b) the curvature of u_2's mean skewness; and (c) the flux of the velocity field's divergence ($\nabla \cdot \mathbf{v} \approx (1-\beta)\tau \mathrm{Tr}(\mathbf{G}^2)$). Physical interpretations of these second-order terms are harder to obtain. However, it is clear from Fig. 6(b) that the second-order corrections are not important in accounting for the mean wall-normal motion of particles for $\tau^+ < 1$.

4.2. Two-way coupled equations

A simple set of two-way coupled equations can be obtained in the limit when both the continuous and dispersed phases can be represented by unique velocity fields as $\mathbf{u}(\mathbf{x},t)$ and $\mathbf{v}(\mathbf{x},t)$. There is no volume transfer between the two phases, so we write volume balance laws for each separately. Eq. (16) implicitly expresses the momentum transfer between the phases, so we need to write only the balance for the total momentum of the system. We express these balances within an arbitrary control volume V with boundary ∂V:

$$\frac{\partial}{\partial t}\int_V c\,\mathrm{d}V + \int_{\partial V} \hat{\mathbf{n}}\cdot(c\mathbf{v})\,\mathrm{d}S = 0, \tag{30}$$

$$\frac{\partial}{\partial t}\int_V (1-c)\,\mathrm{d}V + \int_{\partial V} \hat{\mathbf{n}}\cdot((1-c)\mathbf{u})\,\mathrm{d}S = 0, \tag{31}$$

$$\begin{aligned}\frac{\partial}{\partial t}\int_V \left[c\rho_\mathrm{p}\mathbf{v} + (1-c)\rho_\mathrm{f}\mathbf{u}\right]\mathrm{d}V + \int_{\partial V} \hat{\mathbf{n}}\cdot\left[c\rho_\mathrm{p}\mathbf{v}\mathbf{v} + (1-c)\rho_\mathrm{f}\mathbf{u}\mathbf{u}\right]\mathrm{d}S \\ = \rho_\mathrm{f}\int_V \mathbf{F}\,\mathrm{d}V + \int_V \left[c\rho_\mathrm{p} + (1-c)\rho_\mathrm{f}\right]\mathbf{g}\,\mathrm{d}V,\end{aligned} \tag{32}$$

where $\hat{\mathbf{n}}$ is the unit surface normal, ρ_f and ρ_p are the densities of the continuous and dispersed phases, and $c(\mathbf{x},t)$ is the concentration of the dispersed phase. The two terms on the right-hand side of the last equation represent the surface and volumetric forces on the volume of fluid. The pressure and viscous forces represented by $\mathbf{F}$ should be modified for the two-way interaction. For example, Einstein's viscosity law gives the following form for $\mathbf{F}$:

$$\mathbf{F} = -\nabla p + \left(1+\frac{5}{2}c\right)\nu\Delta\mathbf{u}, \tag{33}$$

which holds for $c \lesssim 0.1$. However, we will ignore this $\mathrm{O}(c)$ modification to the viscosity. For further discussion on constitutive two-phase modeling (see Zhang and Prosperetti (1997) or Drew and Passman (1999)).

The first two of the above equations can be combined to yield the following continuity equation for the continuous phase:

$$\nabla\cdot\mathbf{u} = \frac{\partial c}{\partial t} + \nabla\cdot(c\mathbf{u}). \tag{34}$$

In the limit of small volumetric loading ($c \ll 1$), the fluid continuity equation is usually simplified to the standard incompressibility condition, $\nabla \cdot \mathbf{u} = 0$ The conservation equations of volume and mass also yield the following equation for the concentration field

$$\frac{\partial c}{\partial t} + \nabla \cdot (c\mathbf{v}) = 0. \tag{35}$$

We are now ready to exploit the explicit expansion of particle velocity in terms of the fluid velocity. If the expansion in Eq. (16) is substituted into Eqs. (32) and (35), then standard simplifications result in the following closed system of mass, momentum and concentration balances (valid in the limit of small c):

$$\nabla \cdot \mathbf{u} = 0, \tag{36}$$

$$(1 + (\rho - 1)c)\left(\frac{\mathrm{D}\mathbf{u}}{\mathrm{D}t} - \mathbf{g}\right) = -\nabla p + \nu\Delta\mathbf{u}, \tag{37}$$

$$\frac{\mathrm{D}c}{\mathrm{D}t} = (1 - \beta)\tau\nabla \cdot \left(c\left(\frac{\mathrm{D}\mathbf{u}}{\mathrm{D}t} - \mathbf{g}\right)\right). \tag{38}$$

The effect on the momentum equation is to introduce an effective density, $\rho_{\mathrm{f}}(1 + (\rho - 1)c)$, in agreement with the study of dusty gases (Saffman, 1962; Marble, 1970), Although c is small, ρc may be significant in the dense-particle case, i.e., though volumetric loading is small, mass loading is not. The fact that the chief effect of the particle phase on the momentum equation is simply to modify the effective fluid density can be interpreted as a manifestation of the particles being in equilibrium. Loosely speaking, the particles' velocity is different from the fluid's, but their acceleration is the same.

We ignore higher-order terms both in c and τ in the momentum equation. To obtain more accurate equations, a more sophisticated analysis is required, taking into account the effect of the influence of surrounding particles on a particle's velocity. The effect modifies the velocity of the particle by $\mathrm{O}(c^{1/3})$ (Happel and Brenner, 1965), and is therefore more important to account for than the neglected $\mathrm{O}(c)$ terms and, typically, than the $\mathrm{O}(\tau)$ terms as well.

Finally, there is no mechanism to prevent a buildup toward infinite concentration. This has been observed to cause problems in numerical simulations of the above set of equations (Druzhinin and Elghobashi, 1998). The physical mechanism which prevents $c \to \infty$ is particle–particle collision, which has been completely ignored in the above formulation. The importance of collision in significantly altering the concentration field has recently been addressed by Vance et al. (1999). Inter-particle collision is a hard phenomenon to model. However, for small τ we note that the velocity difference between particles of different response times is always proportional to $\mathrm{D}\mathbf{u}/\mathrm{D}t - \mathbf{g}$. In the frame moving with the fluid velocity, the particles are all moving parallel to each other, so there is some hope of a simple theory. It is not a trivial task however. As was mentioned in Section 2.2, particle collisions result in perturbation away from equilibrium, hence non-equilibrium velocities exist until equilibrium is again established. Also, as particles approach each other, their equations of motion must be modified to account for the effect of local, particle-induced fluid disturbances.

5. Conclusion

For small particle response time τ, one hopes to get away with simply solving for the mixture with a uniform modified density, which takes into account the presence of particles, hence avoiding any detailed coupling between the two phases. However, if τ is large enough that particles tend to either preferentially concentrate or turbophoretically migrate, then the uniform modified density approach for the mixture will fail. One is then forced to treat the concentration c as a field variable and to track the evolution of $c(\mathbf{x}, t)$. The particle velocity field $\mathbf{v}$ must be treated as a field variable as well, else inhomogeneities in c cannot arise. This gives rise to the standard Eulerian approach for particles, where one computes the evolution of $\mathbf{v}(\mathbf{x}, t)$ and $c(\mathbf{x}, t)$ in addition to $\mathbf{u}(\mathbf{x}, t)$. However, for small τ, $\mathbf{v}(\mathbf{x}, t)$ does not differ significantly from the fluid velocity $\mathbf{u}(\mathbf{x}, t)$, and the difference is significant only insofar as it influences the concentration field. Hence, for small τ it is desirable not to compute the particle velocity field explicitly.

The natural thing to do in this situation is to express $\mathbf{v}$ as an expansion in $\mathbf{u}$. Such an expansion has previously been considered by Maxey (1987) and Druzhinin (1995). The first question addressed in this paper is under what conditions a unique particle velocity field can be assumed to exist. For sufficiently large τ, a unique field representation for particle velocity is inappropriate as particles tend to remember their initial conditions for a very long time. On the other hand, for very small particles which move almost with the fluid an Eulerian representation seems appropriate. In Section 2.2 we derived a rigorous upper bound for the particle response time τ below which a unique particle velocity field is appropriate. According to this condition, provided the particle time-scale (τ) normalized by fluid time-scale (as expressed by the inverse of the magnitude of the maximally compressive strain) is less than 1, a unique particle velocity field can be defined. Only in this limit is an Eulerian approach appropriate. We extend the work of Maxey (1987) and Druzhinin (1995) to obtain an expansion for particle velocity in terms of $\mathbf{u}$ and its spatial and temporal gradients, including the effects of added mass, Basset history and Saffman lift terms.

Existence of a unique particle velocity field does not guarantee that the expansion for $\mathbf{v}$ in terms of $\mathbf{u}$ is accurate. In Section 3.2 we considered a database obtained form DNS of particles in turbulent channel flow, and compared the exact velocity of particles (computed by Lagrangian means) to the approximate velocity based on the local fluid quantities. It was observed that the first-order approximation was quite accurate for small τ and provides significant improvement over the zeroth-order approximation (i.e., that the particles follow the local fluid element). The second-order approximation does not yield further improvement consistently over the entire range of τ considered. Thus from a practical point of view, the first-order expansion for particle velocity seems adequate.

In addition to the static tests, in which the exact particle velocity is compared to the zeroth-, first-, and second-order Eulerian approximations at an instant in time, dynamic tests were also performed. Although the first-order approximation was observed to be quite accurate for small τ, there remains the possibility that the small errors may accumulate over time in such a way that the long-term behavior of particle ensembles evolved with the approximate velocity differs from those evolved with the exact velocity. This issue was addressed in Section 3.3, which compares statistics collected over time from two sets of initially identical particles: one evolved with the exact velocity, and the other with the first-order approximate velocity. It was observed that the first-order approximation was able to reproduce all the important statistics quite accurately for particles of

time-scale less than about 1 (in wall units). Particles evolved using the first-order approximate velocity are observed to concentrate in regions of flow vorticity and high strain-rate in the same manner as the exact particles. Analogous results hold for bubbles: the approximately evolved bubbles concentrate in regions of high vorticity just as the exact bubbles do.

The first-order Eulerian expansion has several other nice properties which are otherwise left unaccounted for. The first-order term accurately accounts for turbophoretic migration of particles toward the channel walls (and of bubbles away from the walls). It also predicts the faster-than-fluid streamwise motion of particles near the walls and the streamwise lag of the particles near the channel midplane. The explicit expression for the particle velocity field in terms of the local fluid quantities can be exploited to obtain a consistent two-way coupled formulation. A preliminary investigation of this issue has been addressed in Section 4.2. It is observed that the leading-order effect of two-way coupling on the momentum equation of the continuous phase is to modify the local density, just as in dusty gas formulations. In this sense, the fast Eulerian method forms a natural bridge between the uniform modified density method and the standard Eulerian approach.

Finally, we have only treated monodisperse ensembles of particles. The method becomes even more efficient (relative to the standard Eulerian) for the polydisperse case. For each species of particle tracked, the standard method requires four scalar fields; the fast method requires one. Furthermore, the computation of the correction to $\mathbf{u}$ need only be done for one particle species. The correction has the form $-(1-\beta)\tau(\mathrm{D}\mathbf{u}/\mathrm{D}t-\mathbf{g})$, so once the term $\mathrm{D}\mathbf{u}/\mathrm{D}t-\mathbf{g}$ is computed, velocities for all species of particles may be obtained simply by scaling the correction factor based on the species' response times (τ) and density factors (β).

Acknowledgements

This research was supported by Center for Simulation of Advanced Rockets at the University of Illinois, which is funded by the US Department of Energy through the University California under Subcontract number B341494. Section 3.3 was motivated by discussions with Said Elghobashi during his visit to the University of Illinois in the Fall of 1999.

Appendix A

The semiderivative operator, $\mathrm{d}^{1/2}/\mathrm{d}t^{1/2}$, is useful for expressing the Basset history term in Eq. (3) (Tatom, 1988; Coimbra and Rangel, 1998). It is defined as

$$\frac{\mathrm{d}^{1/2}f}{\mathrm{d}t^{1/2}}=\frac{\mathrm{d}}{\mathrm{d}t}\int_{t_0}^{t}\frac{f(s)}{\sqrt{\pi(t-s)}}\,\mathrm{d}s=\frac{f(t_0)}{\sqrt{\pi(t-t_0)}}+\int_{t_0}^{t}\frac{f'(s)}{\sqrt{\pi(t-s)}}\,\mathrm{d}s. \tag{A.1}$$

(Oldham and Spanier, 1974). Note that the second line automatically provides the constant term which was shown to be necessary by Reeks and McKee (1984).

A point of caution about the semiderivative operator: its composition law is

$$\frac{\mathrm{d}^{1/2}}{\mathrm{d}t^{1/2}}\frac{\mathrm{d}^{1/2}f}{\mathrm{d}t^{1/2}}=\frac{\mathrm{d}f}{\mathrm{d}t}+\frac{C}{(t-t_0)^{3/2}}, \tag{A.2}$$

where C is some constant. If it is desired that $(\mathrm{d}^{1/2}/\mathrm{d}t^{1/2})\mathrm{d}^{1/2}f/\mathrm{d}t^{1/2} = \mathrm{d}f/\mathrm{d}t$, the lower limit t_0 should be set to $-\infty$.

Appendix B

We now prove the convergence theorem stated in Section 2.2. This will provide a rigorous condition for the existence of a unique particle velocity filed (after some initial transient), based on the ratio of particle time-scale to a certain fluid time-scale.

Consider the following equation for the Eulerian velocity field:

$$\frac{\mathrm{d}\mathbf{v}}{\mathrm{d}t} = \frac{1}{\tau}(\mathbf{u}-\mathbf{v}) + \beta\frac{\mathrm{D}\mathbf{u}}{\mathrm{D}t} + (1-\beta)\mathbf{g}. \tag{B.1}$$

This is simply Eq. (4) without the term $\sqrt{\beta/\tau}\mathscr{L}[\mathbf{u}-\mathbf{v}]$. Hence the following analysis accounts for effects such as gravity and added mass, but ignores the Saffman lift and Basset history terms.

Let $\mathbf{v}_1(\mathbf{x},t)$ and $\mathbf{v}_2(\mathbf{x},t)$ be two different velocity fields that satisfy Eq. (B.1). Their difference $\boldsymbol{\delta} = \mathbf{v}_1 - \mathbf{v}_2$ satisfies

$$\frac{\partial\boldsymbol{\delta}}{\partial t} + \mathbf{v}_1\cdot\nabla\boldsymbol{\delta} = -\left(\frac{1}{\tau}\boldsymbol{\delta} + \boldsymbol{\delta}\cdot\nabla\mathbf{v}_2\right). \tag{B.2}$$

Now let $\boldsymbol{\xi}(t)$ be the trajectory of a tracer particle following the velocity field $\mathbf{v}_1$. Then along this trajectory,

$$\frac{\mathrm{d}\boldsymbol{\delta}}{\mathrm{d}t} = -\mathbf{A}\boldsymbol{\delta}, \quad \text{where } \mathbf{A} = \frac{1}{\tau}\mathbf{I} + (\nabla\mathbf{v}_2)^{\mathrm{T}}. \tag{B.3}$$

Here, $\mathbf{I}$ is the identity tensor. Taking the dot product this equation with $\boldsymbol{\delta}$ yields

$$\begin{aligned}&\frac{\mathrm{d}}{\mathrm{d}t}\left(\frac{1}{2}|\boldsymbol{\delta}|^2\right) = -\boldsymbol{\delta}^{\mathrm{T}}\mathbf{A}\boldsymbol{\delta} = -\boldsymbol{\delta}^{\mathrm{T}}\mathbf{B}\boldsymbol{\delta}, \quad \text{where}\\ &\mathbf{B} = \frac{1}{2}(\mathbf{A}+\mathbf{A}^{\mathrm{T}}) = \frac{1}{\tau}\mathbf{I} + \frac{1}{2}\left(\nabla\mathbf{v}_2 + (\nabla\mathbf{v}_2)^{\mathrm{T}}\right).\end{aligned} \tag{B.4}$$

The symmetric tensor $\mathbf{B}$ may be written as $\mathbf{B} = \lambda_1\hat{\mathbf{w}}_1\hat{\mathbf{w}}_1^{\mathrm{T}} + \lambda_2\hat{\mathbf{w}}_2\hat{\mathbf{w}}_2^{\mathrm{T}} + \lambda_3\hat{\mathbf{w}}_3\hat{\mathbf{w}}_3^{\mathrm{T}}$, where λ_j are the eigenvalues of $\mathbf{B}$, and $\hat{\mathbf{w}}_j$ are the corresponding orthonormal set of eigenvectors. The following bound on the time evolution of the difference between the two different particle velocity fields, $\mathbf{v}_1$ and $\mathbf{v}_2$, can then be established as:

$$\begin{aligned}\frac{\mathrm{d}}{\mathrm{d}t}\left(|\boldsymbol{\delta}|^2\right) &= -2\left(\lambda_1|\hat{\mathbf{w}}_1\cdot\boldsymbol{\delta}| + \lambda_2|\hat{\mathbf{w}}_2\cdot\boldsymbol{\delta}| + \lambda_3|\hat{\mathbf{w}}_3\cdot\boldsymbol{\delta}|\right)\\ &\leqslant -2\lambda_{\min}|\boldsymbol{\delta}|^2, \quad \text{and so}\\ \frac{\mathrm{d}}{\mathrm{d}t}(|\boldsymbol{\delta}|^2) &\leqslant -2\left(\frac{1}{\tau} + \sigma_{\min}(\boldsymbol{\xi}(t'),t')\right)|\boldsymbol{\delta}|^2,\end{aligned} \tag{B.5}$$

where $\lambda_{\min}$ is the smallest eigenvalue of $\mathbf{B}$, and $\sigma_{\min}(\mathbf{x},t')$ is the smallest eigenvalue of $\frac{1}{2}(\nabla\mathbf{v}_2 + (\nabla\mathbf{v}_2)^{\mathrm{T}})(\mathbf{x},t')$, which is likely to be negative, corresponding to the most compressive strain of the particle velocity field. Integrating the above inequality from t_0 to $t+t_0$ yields

$$|\boldsymbol{\delta}(t+t_0)|^2 \leqslant |\boldsymbol{\delta}(t_0)|^2 \exp\left(-2\left(\frac{t}{\tau}+\int_{t_0}^{t+t_0}\sigma_{\min}(\boldsymbol{\xi}(t'),t')\,\mathrm{d}t'\right)\right)$$
$$\leqslant |\boldsymbol{\delta}(t_0)|^2 \exp\left(-2t\left(\frac{1}{\tau}+\tilde{\sigma}_{\min}(\boldsymbol{\xi}(t_0);t_0,t)\right)\right), \tag{B.6}$$

where $\tilde{\sigma}_{\min}(\boldsymbol{\xi}(t_0);t_0,t)$ is the smallest value of $\sigma_{\min}$ along the entire trajectory from t_0 to $t+t_0$. The final result on the rate of convergence (or divergence) of the two different velocity fields can now be obtained. For this purpose we define the maximal difference between $\mathbf{v}_1$ and $\mathbf{v}_2$ to be

$$E(t) = \sup_{\mathbf{x}\in R_1(t)} |\mathbf{v}_1(\mathbf{x},t)-\mathbf{v}_2(\mathbf{x},t)|^2, \tag{B.7}$$

where $R_1(t)$ is a material volume for particle velocity field. If we now define the "maximally compressive strain", σ_2, of the particle velocity field over the volume, $R_1(t')$ for $t_0 \leqslant t' \leqslant t+t_0$ as

$$\sigma_2 = \inf_{\mathbf{x}\in R_1(t_0)} \tilde{\sigma}_{\min}(\mathbf{x};t_0,t) = \inf_{\substack{x\in R_1(t_0)\\ t_0\leqslant t'\leqslant t+t_0}} \sigma_{\min}(\mathbf{x},t'), \tag{B.8}$$

then we have the global bound

$$E(t+t_0) \leqslant \exp\left(-2t\left(\frac{1}{\tau}+\sigma_2\right)\right)E(t_0). \tag{B.9}$$

The inequality, $\sigma_{\min}(\boldsymbol{\xi}(t'),t') \geqslant \tilde{\sigma}_{\min}(\boldsymbol{\xi}(t_0);t_0,t) \geqslant \sigma_2$, implied in the above global bound on error may be rather drastic; a tighter bound can be obtained if need be. In any case, provided $-1 < \sigma_2\tau$ a unique particle velocity filed can be considered to exist after transients have decayed.

References

Auton, T.R., Hunt, J.C.R., Prud'homme, M., 1988. The force exerted on a body in inviscid unsteady non-uniform rotational flow. Journal of Fluid Mechanics 197, 241–257.

Balachandar, S., Maxey, M.R., 1989. Methods for evaluating fluid velocities in spectral simulations of turbulence. Journal of Computational Physics 83, 96–125.

Camparaloni, M., Tampieri, F., Trombetti, F., Vittori, O., 1975. Transfer of particles in non-isotropic air turbulence. Journal of Atmospheric Science 32, 565.

Coimbra, C.F.M., Rangel, R.H., 1998. General solution of the particle momentum equation in unsteady Stokes flows. Journal of Fluid Mechanics 370, 53–72.

Drew, D.A., Passman, S.L., 1999. Theory of Multicomponent Fluids. Springer, New York.

Druzhinin, O.A., 1995. On the two-way interaction in two-dimensional particle-laden flows: the accumulation of particles and flow modification. Journal of Fluid Mechanics 297, 49–76.

Druzhinin, O.A., Elghobashi, S., 1998. Direct numerical simulations of bubble-laden turbulent flows using the two-fluid formulation. Physics of Fluids 10, 685–697.

Druzhinin, O.A., Elghobashi, S., 1999. On the decay rate of isotropic turbulence laden with microparticles. Physics of Fluids 11, 602–610.

Elghobashi, S., Truesdell, G.C., 1992. Direct simulation of particle dispersion in a decaying isotropic turbulence. Journal of Fluid Mechanics 242, 655–700.

Ferry, J., Balachandar, S., 1999. Estimate of the effect of flow inhomogeneity of forces on particles in a wall-bounded flow. Physics of Fluids.

Happel, J., Brenner, H., 1965. Low Reynolds Number Hydrodynamics. Prentice-Hall, Englewood Cliffs, NJ.
Ling, W., Chung, J.N., Troutt, T.R., Crowe, C.T., 1998. Direct numerical simulation of a three-dimensional temporal mixing layer with particle dispersion. Journal of Fluid Mechanics 358, 61–85.
Marble, F.E., 1970. Dynamics of dusty gases. Annual Review of Fluid Mechanics 2, 397–446.
Maxey, M.R., 1987. The gravitational settling of aerosol particles in homogeneous turbulence and random flow fields. Journal of Fluid Mechanics 174, 441–465.
Maxey, M.R., Riley, J.J., 1983. Equation of motion for a small rigid sphere in a non-uniform flow. Physics of Fluids 26, 883–889.
McLaughlin, J.B., 1991. Inertial migration of a small sphere in linear shear flows. Journal of Fluid Mechanics 224, 261–274.
Meiburg, E., Wallner, E., Psagella, A., Riaz, A., Härtel, C., Necker, F., 1999. Vorticity dynamics of dilute, two-way coupled particle laden mixing layers Technical Report CMS-99-7, Center for Modeling and Simulation, University of Southern California, Los Angeles, CA 90089.
Oldham, K.B., Spanier, J., 1974. The Fractional Calculus. Academic Press, New York.
Reeks, M.W., 1983. The transport of discrete particles in inhomogeneous turbulence. Journal of Aerosol Science 14, 729–739.
Reeks, M.W., McKee, S., 1984. The dispersive effects of Basset history forces on particle motion in a turbulent flow. Physics of Fluids 27, 1573–1582.
Saffman, P.G., 1962. On the stability of laminar flow of a dusty gas. Journal of Fluid Mechanics 13, 120–128.
Saffman, P.G., 1965. The lift on small sphere in a slow shear flow. Journal of Fluid Mechanics 22, 385–400.
Squires, K.D., Eaton, J.K., 1991. Preferential concentration of particles by turbulence. Physics of Fluids A 3, 1169–1178.
Tatom, F.B., 1988. The Basset term as a semiderivative. Applied Scientific Research 45, 283–285.
Vance, M.W., Squires, K.D., Simonin, O., 1999. On the effect of collisions in gas-solid turbulent channel flow. In: APS-DFD Conference.
Wang, Q., Squires, K.D., Chen, M., McLaughlin, J.B., 1997. On the role of the lift force in turbulence simulations of particle deposition. International Journal of Multiphase Flow 23, 749–763.
Williams, F.A., 1985. Combustion Theory. Benjamin/Cummings, San Francisco.
Yeung, P.K., Pope, S.B., 1989. Lagrangian statistics from direct numerical simulations of isotropic turbulence. Journal of Fluid Mechanics 207, 531–586.
Zhang, D.Z., Prosperetti, A., 1997. Momentum and energy equations for disperse two-phase flows and their closure for dilute suspensions. International Journal of Multiphase Flow 23, 425–453.
Zhou, J., Adrian, R.J., Balachandar, S., 1996. Autogeneration of near-wall vortical structures in channel flow. Physics of Fluids 8, 288–290.
Zhou, J., Adrian, R.J., Balachandar, S., Kendall, T.M., 1999. Mechanisms for generating coherent packets of hairpin vortices in channel flow. Journal of Fluid Mechanics 387, 353–396.
Zhou, Y., Wexler, A.S., Wang, L.-P., 1998. On the collision rate of small particles in isotropic turbulence. II. Finite inertia case. Physics of Fluids 10, 1206–1216.